Facile Synthesis, Crystal Growth, Quantum Chemical Studies of Electronic Structure and of the Profoundly Persuasive NLO Organic Crystal: Ethyl 4-[*N*,*N*-*bis*(*p*-toluenesulfonyl)]- Aminobenzoate

[1]Sana Mazhar, [2,3]Muhammad Khalid*, [4]Muhammad Nawaz Tahir, [1]Muhammad Haroon, [1]Tashfeen Akhtar*, [5]Muhammad Usman Khan, [2]Farrukh Jaleel, [6]Muhammad Aslam

[1]*Department of Chemistry, Mirpur university of Science and Technology (MUST), Mirpur-1250 (AJK), Pakistan.*

[2]*Department of Chemistry, Khwaja Fareed University of Engineering & Information Technology, Rahim Yar Khan 64200, Pakistan.*

[3]*Department of Chemistry, University of Education Lahore Faisalabad Campus, Faisalabad 38000, Pakistan.*

[4]*Department of Physics, University of Sargodha, Sargodha 40100, Punjab, Pakistan.*

[5]*Department of Applied Chemistry, Government College University, Faisalabad 38000, Pakistan.*

[6]*Department of Chemistry, University of Education, Lahore 54000, Pakistan.*

khalid@iq.usp.br*

(Received on 26th December 2017, accepted in revised form 18th May 2018)

Summary: In the present work, we synthesized Ethyl-4-[*N*,*N*-*bis* (*p*-toluene sulfonyl)amino]benzoate crystal and structurally characterized by X-ray diffraction (XRD) method. The optimized geometry and vibration wave numbers of the compound investigated was obtained by performing density functional theory (DFT) computations at the M06-2X level of theory and with the 6-311+G(d,p) basis set. The DFT findings show good agreement with the experimental XRD data. Natural bond orbital (NBO) study was performed at the M06-2X/6-311+G(d,p) level to find the stability due to charge delocalization and hyperconjugative interactions. Charge transfer properties and chemical activities at different sites of the synthesized compound was quantitatively determined by performing frontier molecular orbital (FMO) analysis and molecular electrostatic potential (MEP) surfaces at the M06-2X level of theory with 6-311+G(d,p) basis set. The global reactivity parameters were explored with use of the energy of the FMOs. These descriptors predicted the stability of the investigated molecule by revealing the larger hardness and less softness values. Nonlinear optical (NLO) properties was computed at the M06-2X level of theory and 6-311+G(d,p) basis set combination which is observed larger as compared to the urea molecule indicating the considerable NLO character.

Keywords: Bissulphonylation, X-ray diffraction, Density Functional Theory, Natural Bond Orbital analysis, Frontier Molecular Orbital, Nonlinear optical properties.

Introduction

The immense biological activities of sulphonamides make them a target of choice for the synthetic chemists. In medicinal chemistry and drug industry, importance of sulphonamides has not been ignored [1-3]. They are the first active chemotherapeutic agents used to prevent and cure the bacterial infections in human [4-7]. They exhibit antibacterial, antimicrobial, antiviral, anti-inflammatory [8], anti-cancer [9-11] activities and are also used as HIV protease inhibitors [12]. The hypoglycemic, diuretics [13] and anti-metabolite [14] activities of sulphonyl derivatives are also reported. In organic synthesis, aryl sulfonyl halides are used as protecting groups for alcohols and amines due to their ease of formation and high stability [15]. Sulphonamides are usually synthesized by the reaction of primary or secondary amines or ammonia with sulphonyl halides under basic conditions [16]. It is difficult to synthesize bis-sulphonamides due to the steric hindrance of phenyl groups of sulphonyl moiety. In an attempt to make the sulphonylation of 4-amino-benzoate, we obtained the product with relatively higher R_f value and initial characterization suggested by the possibility of bis-sulphonylation, which was confirmed by the crystal structure of the compound investigated.

Variety of conjugated organic materials to be used in optical devices has been synthesized with large optical linearities [17-20]. Telecommunication requires high nonlinear optical (NLO) materials for electro-optical switching elements and information processing. In optical fibers, the electrons of metallic conductor are replaced by photons now. The capacity of multi wavelength optical communication increases by order of magnitudes of an optical network as compared to the electronic communication. In the last twenty years, plenty of conjugated organic organometallics and inorganic molecules have been studied to find out suitable NLO materials [21-23].

*To whom all correspondence should be addressed.

From literature survey, it reveals that the experimental and DFT computations of the synthesized molecule have not been reported so far. Therefore, In this paper, synthesis and crystal structure of the Ethyl 4-[*N,N-bis*(*p*-toluene sulfonyl)]aminobenzoate (scheme 1) was examined. The synthesized compound was characterized through X-ray single crystal study and subjected to DFT studies to explore more about geometry and electronic properties. For the prediction of molecular properties, frontier molecular orbital (FMO) analysis was carried out. Natural bond orbital (NBO) analysis was performed to investigate the bond strength, shift in charge and stability of the molecule. Dipole moment, polarizability, first and second hyperpolarizability of the synthesized molecule has been calculated to show nonlinear optical (NLO) properties. Molecular electrostatic potential (MEP) surfaces were investigated for the estimation of nucleophilic as well as electrophilic sites of the synthesized molecule. Furthermore, thermodynamic parameters calculations have been performed to study the variations in thermodynamic functions as a function of temperature.

Experimental

Reagents and instrumentation

All reagents used were of high purity grade and used without further purification. Ethyl 4-aminobenzoate and p-toluenesulphonyl chloride were products of Merck, Germany. The completion of the reaction was observed by thin layer chromatography (TLC) using pre-coated silica gel 60HF254aluminum sheet. Gallen Kemp melting point apparatus was used to determine the melting point and is uncorrected. The crystal structure was determined using Bruker Kappa APEX II CCD diffractometer.

Synthesis of Ethyl 4-[N,N-bis(p-toluenesulfonyl)]aminobenzoate

Dichloromethane (15mL), ethyl4-aminobenzoate (0.001 moles) and triethylamine (TEA) (0.003moles, 3eq) were added in a round bottomed flask and reaction mixture was stirred at 0˚C for nearly 15 minutes. Then, solution of *p*-toluenesulphonyl chloride (0.0015 moles, dichloromethane 10mL) was added drop wise to the reaction mixture and the resulting mixture was allowed to reflux for 5 hours. The reaction was monitored by TLC at regular intervals. After completion, reaction mixture was added into ice cold water and neutralized by adding 2N HCl. The crude product obtained was washed with ammonium chloride solution (3× 20mL) to remove unreacted amine. The combined organic layers were concentrated on rotary evaporator followed by re-crystallization from methanol to get pure product. Yield: 85%, m.p: 210-212°C.

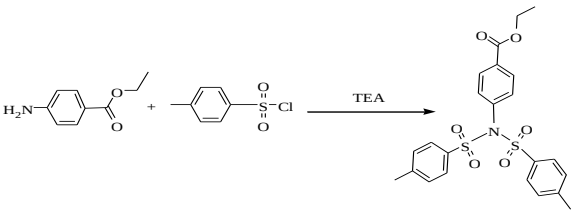

Scheme-1: Synthesis of ethyl 4-[*N,N-bis*(p-toluenesulfonyl)amino]benzoate.

Computational procedure

All the computational calculations were performed on the base of DFT [24] utilizing the Gaussian 09 program [25]. From crystal structure, the initial geometry of the synthesized compound was obtained. The geometry was fully optimized at M06-2X level applying the 6-311+G(d,p) basis set without any symmetry restriction. Subsequently, the obtained positive frequencies make clear that the geometry was entirely optimized and corresponds to the true minimum in the potential energy surface. FMOs, NBO, NLO and MEP analysis were also performed using M06-2X/6-311+G(d,p) level of theory. The Avogadro [26], ChemCraft [27] and GaussView 5.0 [28] programs were employed to organize input files and interpret the output files results.

Results and Discussion

XRD study

The single crystal of the synthesized compound was verified using Bruker Kappa APEX II CCD diffractometer with a graphite monochromator MoKα radiation (λ = 0.71073 Å) at room temperature. Several different programs like, *SAINT* and *APEX 2*were used for cell refinement, data reduction and data collection [29]. *SHELXS97* program was used to solve the structure and for the structural refinement [30]. For molecular graphics *ORTEP-3* for Windows [31], Mercury 3.6 programe and *PLATON* were used [32].

Table-1: Single crystal XRD parameters of synthesized molecule.

Crystal data	*SHELX*
Chemical formula	$C_{23}H_{23}NO_6S_2$
M_r	473.54
Crystal system, space group	Monoclinic, $P2_1/n$
Temperature (K)	296
a, *b*, *c* (Å)	12.8788 (12), 15.0426 (15), 23.753 (2)
β (°)	98.511 (4)
V (Å^3)	4551.0 (8)
Z	8
Radiation type	Mo *Kα*
μ (mm^{-1})	0.27
Crystal size (mm)	0.40 × 0.22 × 0.20
Data collection	
Diffractometer	?
Absorption correction	–
No. of measured, independent and observed [$I > 2\sigma(I)$] reflections	26168, 9812, 4994
R_{int}	0.046
$(\sin \theta/\lambda)_{max}$ (Å^{-1})	0.639
Refinement	
$R[F^2 > 2\sigma(F^2)]$, $wR(F^2)$, *S*	0.061, 0.196, 0.99
No. of reflections	9812
No. of parameters	583
H-atom treatment	H-atom parameters constrained
$\Delta\rho_{max}$, $\Delta\rho_{min}$ (e Å^{-3})	0.35, −0.34

Computer programs: *SHELXL2014/7* (Sheldrick, 2014).

In the synthesized compound, two independent molecules make the asymmetric unit. The two molecules differ each other geometrically. In the first molecule, the aniline moiety A (C4-C9/N1), toluene groups B (C10-C16) and C (C17-C23) are planar with r. m. s. deviations of 0.0257, 0.0165 and 0.0047 Å, respectively. 29.86(11)°, 35.75 (9)° and 41.91 (8)° are the dihedral angle among *A*/*B*, *A*/*C* and *B*/*C* respectively. The sulfonyl groups D (S1/O3/O4) and E (S2/O5/O6) are of course planar. The dihedral angle of these sulfonyl groups with adjacent toluene groups *i.e* B/D and C/E is 42.79 (19)° and 51.75 (16)°, respectively. In the second molecule, the aniline moiety F (C4-C9/N1), toluene groups G (C10-C16) and H (C17-C23) are planar with r. m. s. deviations of 0.0394, 0.0047 and 0.0108 Å, respectively. 26.42(8)°, 35.04 (11)° and 39.00 (10)° are the dihedral angle among *F*/*G*, *F*/*H* and *G*/*H* respectively. The sulfonyl groups I (S3/O9/O10) and J (S4/O11/O12) are of course planar. The dihedral angle of these sulfonyl groups with adjacent toluene groups *i.e* G/I and H/J is 20.22 (17)° and 45.14 (17)°, respectively. Moreover the ethyl formate moieties attached to anilinic groups behave differently, one is planar and the other is not. The molecules are mainly stabilized due to van der waals forces. The projectional diagram along the a-axis is shown below.

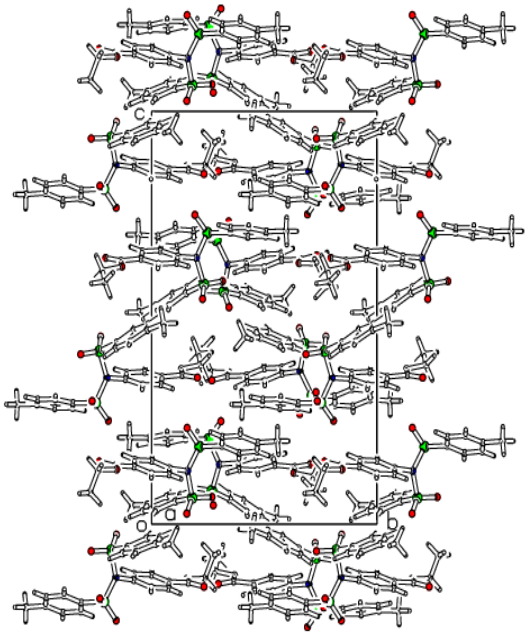

Fig. 1: Projection diagram along a-axis.

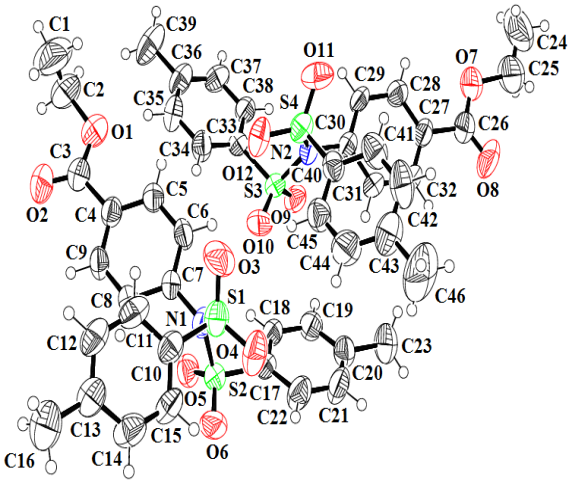

Fig. 2: The asymmetric unit of the synthesized compound with thermal ellipsoids at 50 % probability level. The H-atoms are drawn as small circles of arbitrary radii.

Computational optimization and geometrical structure

Both structures attained from XRD analysis and through geometrical optimization at the at the DFT/M06-2X/6-311+G(d,p) level have been displayed in Fig. 2 and 3.

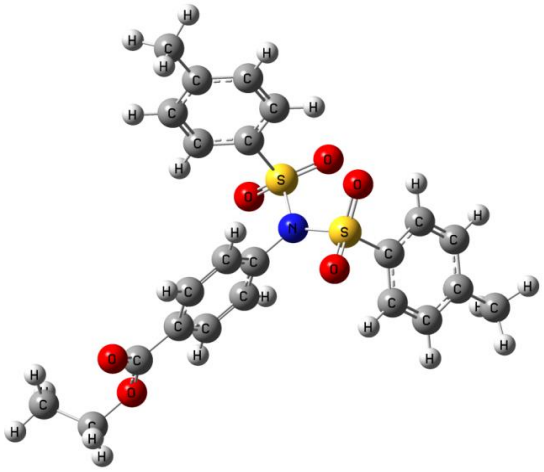

Fig. 3: Optimized geometry of synthesized molecule M06-2X /6-311+G(d,p) level.

The comparison of calculated bond lengths and bond angles obtained from DFT and XRD studies have been presented in Table-2 which illustrate that the XRD and DFT calculated bond lengths and bond angles are associated adequately. These bond lengths and bond angles were deviated in the range of 0.24 ± 0.02 Å and 3° ± 2° respectively. The maximum deviation in the bond length 0.241 Å was observed for C(10)-C(11) while 2.6° deviation in the bond angle was found in O(6)-S(1)-N(9). Both DFT and XRD calculated bond lengths of the C–C bond in the benzene ring of synthesized molecule were observed in the range of 1.384-1.395Å and 1.365-1.385 Å respectively. These ranges are smaller than the C-C (1.540 Å) and larger than the C=C (1.340 Å) bond lengths [33]. The bond length between carbon and oxygen atoms calculated through DFT is calculated to be 1.339Å and 1.203Å for O(3)-C(12) and O(4)-C(12) respectively, while XRD calculated bond length for O(3)-C(12) and O(4)-C(12) is observed as 1.313Å and 1.188Å respectively. Divergence in bond length for S(1)-O(5), S(1)-O(6), S(2)-O(7) and S(2)-O(8) is observed as 1.433, 1.432, 1.434 and 1.433Å through DFT while XRD calculations give deviation as 1.421, 1.414, 1.421 and 1.414Å respectively. The calculated bond angles tabulated in Table-2 between O(5)-S(1)-O(6) and O(7)-S(2)-O(8) of SO_2 are observed at 121.8, 121.6° (DFT) and 120.5, 120.5° (EXP) respectively. Similarly the bond angle in the CO_2 molecule between O(3)-C(12)-O(4) is found to be 123.7° (DFT) and 123.2° (EXP). The bond angle of the bridge S(1)-N(9)-S(2) that connect the benzene rings is identified as 121.4° (DFT) and 122.7°(EXP) respectively. Comparative analysis of the geometric data of the investigated molecule indicates that, except for few exceptions, experimentally determined parameters illustrate good agreement with the all computed parameters.

Table-2: Comparison of selected bond lengths (Å), angles (°) using M06-2X/6-311+G(d,p) and X-ray diffraction method.

Bond length (A°)	M06-2X	XRD	Bond angle (°)	M06-2X	XRD
R(1-5)	1.433	1.421	A(5-1-6)	121.8	120.5
R(1-6)	1.432	1.414	A(5-1-9)	105.2	103.4
R(1-9)	1.695	1.690	A(5-1-19)	108.2	109.5
R(1-19)	1.761	1.738	A(6-1-9)	106.1	108.7
R(2-7)	1.434	1.421	A(6-1-19)	109.9	109.0
R(2-8)	1.433	1.414	A(9-1-19)	104.0	104.5
R(2-9)	1.706	1.665	A(1-9-2)	121.4	122.7
R(2-26)	1.761	1.728	A(1-9-16)	118.1	119.4
R(3-11)	1.438	1.455	A(1-19-20)	118.9	120.5
R(3-12)	1.339	1.313	A(1-19-24)	119.4	119.1
R(4-12)	1.203	1.188	A(7-2-8)	121.6	120.5
R(9-16)	1.433	1.437	A(7-2-9)	104.1	105.8
R(10-11)	1.514	1.273	A(7-2-26)	108.6	108.4
R(12-13)	1.492	1.481	A(8-2-9)	108.1	106.6
R(13-14)	1.392	1.390	A(8-2-26)	109.4	110.3
R(13-18)	1.392	1.373	A(9-2-26)	103.5	103.9
R(14-15)	1.385	1.369	A(2-9-16)	119.4	117.2
R(15-16)	1.388	1.367	A(2-26-27)	118.4	119.5
R(16-17)	1.390	1.385	A(2-26-31)	119.9	120.5
R(17-18)	1.384	1.374	A(11-3-12)	116.0	116.5
R(19-20)	1.388	1.377	A(3-11-10)	111.2	113.6
R(19-24)	1.388	1.383	A(3-12-4)	123.7	123.2
R(20-21)	1.386	1.368	A(3-12-13)	112.6	112.7
R(21-22)	1.394	1.376	A(4-12-13)	123.7	124.1
R(22-23)	1.395	1.380	A(9-16-15)	119.0	120.2
R(22-25)	1.504	1.511	A(9-16-17)	119.9	119.2
R(23-24)	1.385	1.367	A(12-13-14)	122.0	122.1
R(26-27)	1.388	1.377	A(12-13-18)	117.6	118.1
R(26-31)	1.386	1.379	A(14-13-18)	120.4	119.8
R(27-28)	1.385	1.363	A(13-14-15)	119.8	119.9
R(28-29)	1.394	1.373	A(13-18-17)	120.0	120.1
R(29-30)	1.394	1.371	A(14-15-16)	119.5	120.1
R(29-32)	1.504	1.501	A(15-16-17)	121.1	120.4
R(30-31)	1.385	1.365	A(16-17-18)	119.3	119.6
			A(20-19-24)	121.7	120.4
			A(19-20-21)	118.7	119.5
			A(19-24-23)	118.6	119.0
			A(20-21-22)	121.0	121.0
			A(21-22-23)	118.8	118.7
			A(21-22-25)	120.6	120.9
			A(23-22-25)	120.6	120.4
			A(22-23-24)	121.2	121.3
			A(27-26-31)	121.8	119.9
			A(26-27-28)	118.8	119.2
			A(26-31-30)	118.5	119.6
			A(27-28-29)	120.9	121.8
			A(28-29-30)	118.8	118.2
			A(28-29-32)	120.7	120.8
			A(30-29-32)	120.5	121.0
			A(29-30-31)	121.2	121.3

NBO analysis

NBO analysis is an efficient technique that effectively describes the delocalization of electron density and intramolecular rehybridization. It offers suitable foundations to study intramolecular hydrogen bonding and charge transfer among the filled and vacant orbitals by second order Fock matrix [34, 35]. Hence NBO analysis were carried out at the M06-2X level of theory and with the 6–311+G(d,p) basis set by taking into account all probable interactions among donor to acceptor using second-order Fock matrix [36] equation given in the supplementary material and the possible intensive interactions are given in Table-3.

Table-3: Natural bond orbital (NBO) analysis using second-order perturbation theory.

Donor(i)	Type	Acceptor(j)	Type	E(2)[a] [kJ/mol]	E(j)–E(i)[b] [a.u.]	F(i,j)c [a.u.]
C18 – C19	π	C21 – C23	π *	29.46	0.35	0.091
C18 – C19	π	C24 – C26	π *	31.81	0.31	0.090
C21 – C23	π	C24 – C26	π *	29.43	0.31	0.087
C24 – C26	π	C21 – C23	π *	30.69	0.35	0.091
C28 – C29	π	C31 – C33	π *	23.54	0.39	0.086
C28 – C36	σ	C31 – H32	σ*	35.83	0.17	0.070
C31 – C33	π	C34 – C36	π *	12.31	0.75	0.087
C33 – C34	σ	C31 – H32	σ*	16.30	0.14	0.043
C34 – C36	π	C31 – C33	π *	32.35	0.36	0.096
C42 – C43	π	C45 – C47	π *	24.67	0.35	0.084
C45 – C47	σ	S1 – N9	σ*	24.68	0.44	0.100
C45 – C47	σ	C31 – H32	σ*	213.21	0.15	0.159
C45 – C47	π	C42 – C43	π *	40.07	0.33	0.103
C47 – C48	σ	C31 – H32	σ*	247.27	0.14	0.176
C10 – H11	σ	O3 – C14	σ*	0.56	0.89	0.020
C48 – C50	π	C45 – C47	π *	33.21	0.33	0.094
O4 – C17	π	C45 – C47	π *	33.21	0.33	0.094
C52 – H53	σ	S1 – N9	σ*	292.16	0.23	0.251
C52 – H53	σ	O4 – C17	σ*	73.49	0.89	0.229
C52 – H53	σ	C28 – C29	π *	512.34	0.14	0.263
C52 – H54	σ	S1 – N9	σ*	303.01	0.23	0.253
C52 – H54	σ	C28 – C29	π *	528.12	0.13	0.264
C52 – H55	σ	S1 – N9	σ*	1458.51	0.13	0.351
C52 – H55	σ	O4 – N17	σ*	223.39	0.79	0.376
C52 – H55	σ	C28 – C29	π *	5344.29	0.04	0.435
O3	LP(2)	O4-C17	?*	57.43	0.44	0.144
O4	LP(2)	O3-C17	σ*	38.21	0.77	0.155
O4	LP(2)	C17-C18	σ*	20.50	0.82	0.118
O5	LP(2)	S1-N9	σ*	127.11	0.03	0.053
O5	LP(3)	S1-N9	σ*	843.10	0.02	0.109
O6	LP(2)	S1-N9	σ*	203.39	0.03	0.067
O6	LP(3)	S1-N9	σ*	643.26	0.02	0.101
O7	LP(2)	S2-N9	σ*	43.75	0.38	0.118
O8	LP(2)	S2-C42	σ*	21.05	0.56	0.097
O8	LP(3)	S2-N9	σ*	32.08	0.38	0.101
O8	LP(3)	S2-N9	σ*	32.08	0.38	0.101

[a]Energy of hyper conjugative interaction (stabilization energy).
[b] Energy difference between donor and acceptor i and j NBO orbital.
[c]Fock matrix element between i and j NBO orbital.

The most credible transitions takes place in our studied systems is σ(C52-H55)→π*(C28-C29) with stabilization energy value 5344.29 kJ/mol. This is the substantial stabilization energy value observed in the synthesized molecule (Table-3). On the other hand, σ(C10-H11)→σ*(O3-C14) transition indicates the weak interaction between donor (σ) and acceptor (σ*) due to their least stabilization energy value 0.56 kJ/mol. The occurrence of conjugation can be judged with the examination of π→π* interactions. Some important transitions that represent conjugation in investigated molecule are π(C18-C19)→π*(C24-C26), π(C21-C23)→π*(C24-C26), π(C24-C26)→π*(C21-C23), π(C28-C29)→ π*(C31-C33), π (C34-C36)→ π*(C31-C33), π(C42-C43)→ π*(C45-C37) and π(C48-C50)→ π*(C45-C47) which led to the stabilization energies are found to be 31.81, 29.43, 30.69, 23.54, 32.35, 24.67 and 33.21 kJ mol^{-1} respectively (Table-3). Some other transition involving large stabilization energies are σ(C52-H55)→ π*(S1-N9), σ(C52-H53)→σ*(S1-N9), σ(C52-H53)→σ*(O4-C17), σ(C52-H53)→ π*(C28-C29), σ(C52-H54)→ σ*(S1-N9), σ (C52-H54)→ π*(C28-C29 and σ(C52-H55)→ σ*(O4-N17) with energy values 1458.51, 292.16, 73.49, 512.34, 303.01, 528.12, and 223.39 kJ/mol respectively. In case of the resonance, the massive stabilization energy values for the transition LP(O5)→σ*(S1-N9) is 843.10 kJ/mol respectively. Furthermore, some transitions such as LP(O6)→σ*(S1-N9), LP(O6)→σ*(S1-N9) and LP(O5)→σ*(S1-N9) also contain large stabilization energy values 643.26, 203.39, and 127.11 kJ/mol respectively (Table-3). From above discussion, it is apparent that extended conjugation is present in the synthesized molecule. Intra-molecular charge transfer generates strong intra-molecular hyper conjugative interactions which leads to the stabilization of compound investigated.

FMO analysis

FMO analysis have been considered excellent in predicting the chemical stability of the molecules under investigation [37]. The lowest unoccupied molecular orbital (LUMO) and highest occupied molecular orbital (HOMO) are very important quantum orbitals. Usually, the LUMO expresses the capacity of accepting an electron while HOMO denotes the electron donation ability [38]. The HOMO-LUMO energy gap is an important parameter for predicting the chemical reactivity and dynamic stability of molecules [39]. In order to have photophysical insight of the synthesized molecule, HOMO and LUMO levels and their energies

are calculated using M06-2X/6-311+G(d,p) method and energies are shown in Table-4.

Table-4: Computed energy values for the synthesized molecule in gas phase.

MO(s)	*E* (eV)	Δ*E* (e*V*)
HOMO	**-8.395**	**7.412**
LUMO	**-0.983**	
HOMO-1	**-8.676**	**8.055**
LUMO+1	**-0.621**	
HOMO-2	**-8.810**	**8.542**
LUMO+2	**-0.268**	
HOMO-3	**-8.818**	**8.747**
LUMO+3	**-0.071**	

E= energy, Δ*E* (e*V*) = E_{LUMO}-E_{HOMO}

Four significant molecular orbital pairs HOMO, LUMO as well as HOMO-1, LUMO+1, HOMO-2, LUMO+2 and HOMO-3, LUMO+3 were explored and their calculated energy values obtained -8.395, -0.983, -8.676, -0.621, -8.810, -0.268 , -8.818 and -0.071 (eV) respectively. The contour surfaces of these FMOs are exposed in Fig. 4 with energy gap values observed 7.412, 8.055, 8.542 and 8.747 eV (see Table-4 and Fig. 4).

Molecules with higher energy gap (E_{LUMO}-E_{HOMO}) are considered to be chemically hard molecules with higher kinetic stability and less chemical reactivity. In contrast, more stable, less reactive and soft molecules are those having small (E_{LUMO}-E_{HOMO}) frontier orbital energy gap. The energies and frontier orbital gap of HOMO-LUMO contribute vital part in the estimation of internal charge transfer (ICT), chemical reactivity and stability of the systems by predicting global reactivity descriptors [40-43]. Global reactivity parameter like electro negativity (*X*), electrophilicity index (ω), chemical potential (μ), global softness (*S*), ionization potential (*IP*), global hardness (η) and electron affinity (*EA*) are calculated using equations given in the supplementary material and results are expressed in Table-5.

Due to the electron donating and accepting ability of HOMO and LUMO, these are directly related to the ionization potential and electron affinity respectively. Table-5 shows that the ionization potential value of compound investigated is much higher than the electron affinity value which indicate that the synthesized molecule might act as better donor molecule. Electron affinity value was found positive which indicate that the synthesized molecule might participate in charge transfer reactions. Electronegativity value of the synthesized compound was found to be 4.689. The electrophilicity index is often used to measure the lowering of energy because of maximum electron flow among HOMO and LUMO. The electrophilicity index of our compound was found to be 2.96. The global hardness value of the synthesized molecule was found to be 3.706 (e*V*) which is 28 times greater than the global softness (*S*) value 0.1314(e*V*). The greater hardness value as compared to the softness value is due to large E_{HOMO}–E_{LUMO} energy difference. Therefore, the synthesized compound has high chemical stability. These findings suggest that the synthesized molecule is a hard and stable molecule with better donating capabilities.

Table-5: Ionization potential (*IP*), electron affinity (*EA*), electro negativity (*X*) chemical potential (μ) global hardness (η) global softness (*S*) and global electrophilicity (ω).

	A	B	C	D
***I* (e*V*)**	**8.395**	**8.676**	**8.81**	**8.818**
***A*(e*V*)**	**0.983**	**0.621**	**0.268**	**0.071**
***X* (e*V*)**	**4.689**	**4.6485**	**4.539**	**4.4445**
μ (e*V*)	**-4.689**	**-4.6485**	**-4.539**	**-4.4445**
η (e*V*)	**3.706**	**4.0275**	**4.271**	**4.3735**
***S* (e*V*)**	**0.134916**	**0.124146**	**0.117069**	**0.114325**
ω (e*V*)	**2.966368**	**2.682626**	**2.411908**	**2.258326**

A= HOMO & LUMO; B= HOMO-1& LUMO+1; C= HOMO-2 & LUMO+2; D= HOMO-3 & LUMO+3

Nonlinear optical (NLO) properties

At the present time, nonlinear optical (NLO) materials based on organic compounds have gained mounting attention by scientists due to their facile synthesis, low price, easy fabrication, structural modifications and their diverse applications in photonics, electronics, optoelectronic technologies and especially in nonlinear optics [44, 45]. The structure of organic compounds showing NLO behavior is recognized on the basis of asymmetric polarization. It is directed by substitution of suitable electron contributor and withdrawing units on appropriate position. The NLO behavior is increased by enhancing the electron withdrawing and contributor group's effectiveness connected to the π-conjugated system [46, 47] . NLO properties of the investigated molecule have been studied in gas phase at the M06-2X/6-311+G(d,p) level.

Average polarizability, first hyperpolarizability (β_{tot}) and second hyperpolarizability (γ) is calculated using following equation 1-3 and results are given in Table-6.

$$<\alpha>=1/3(\alpha_{xx}+\alpha_{yy}+\alpha_{zz}) \quad (1)$$

$$\beta_{tot}=[(\beta_{xxx}+\beta_{xyy}+\beta_{xzz})^2+(\beta_{yyy}+\beta_{yzz}+\beta_{yxx})^2+(\beta_{zzz}+\beta_{zxx}+\beta_{xyz})^2]^{1/2} \quad (2)$$

$$\langle\Upsilon\rangle=\frac{1}{5}\left(\Upsilon_{xxxx}+\Upsilon_{yyyy}+\Upsilon_{zzzz}+2[\Upsilon_{xxyy}+\Upsilon_{yyzz}+\Upsilon_{xxzz}]\right) \quad (3)$$

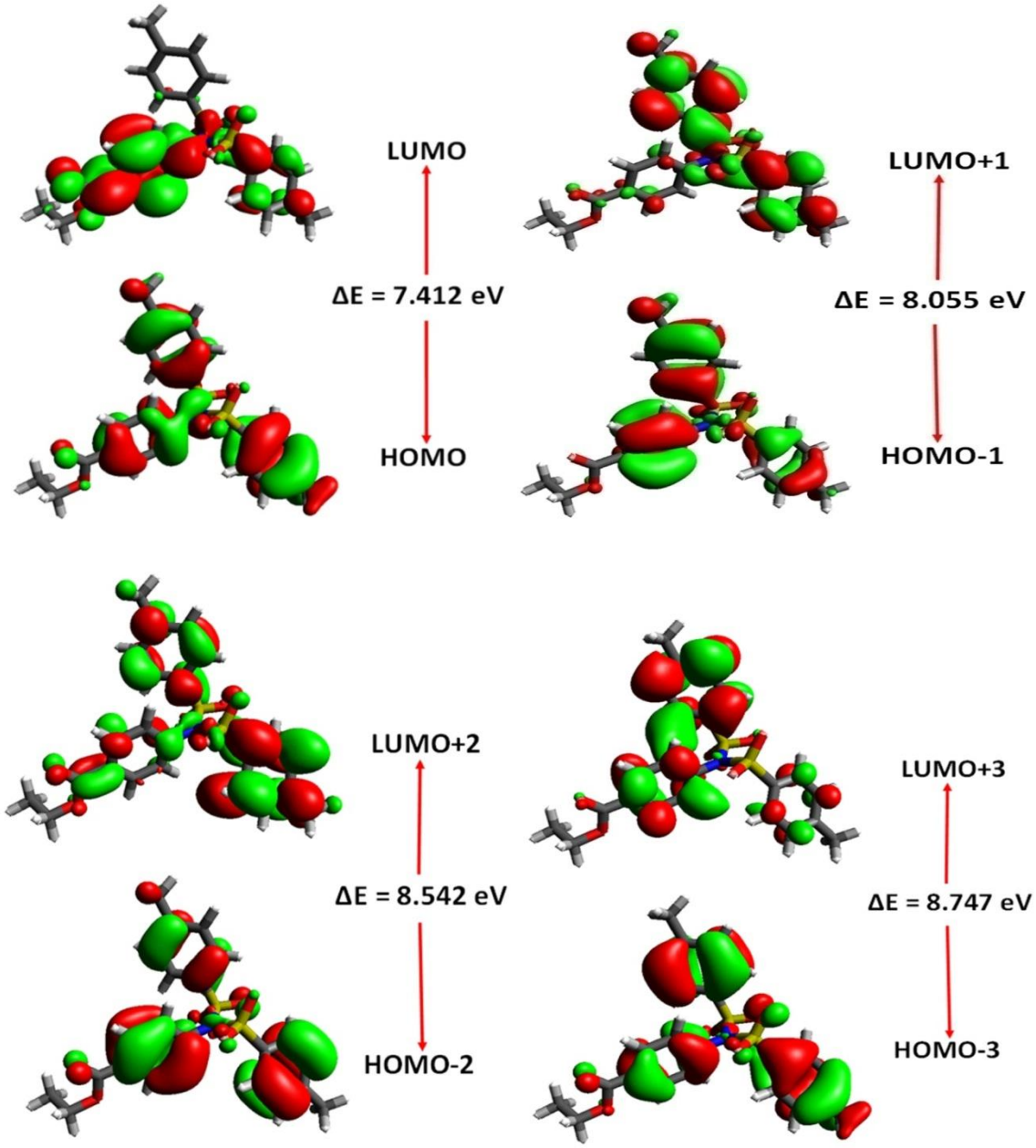

Fig. 4: Frontier molecular orbitals of the synthesized molecule.

Table-6: The dipole moment, polarizability, first and second hyperpolarizability values calculated at M06-2x/6-311+G (d, p).

μ_x	-0.7563	β_{xxx}	-1.1238	γ_{xxxx}	-11704.5324
μ_y	-1.0700	β_{xyy}	-12.7181	γ_{yyyy}	-8095.0889
μ_z	-1.4382	β_{xzz}	-21.2771	γ_{zzzz}	-1599.3271
μ_{tot}	1.9456	β_{yyy}	47.8623	γ_{xxyy}	-3098.5617
α_{xx}	-182.9422	β_{xxy}	-132.7262	γ_{zzxx}	-2497.2849
α_{yy}	-157.1937	β_{yzz}	-3.7284	γ_{yyzz}	-1815.6672
α_{zz}	-219.0088	β_{zzz}	-1.3937	γ x10^{-28} (esu)	-2.10
α_{xy}	-8.5991	β_{xxz}	-79.4752		
α_{xz}	4.5320	β_{yyz}	12.1663		
α_{yz}	9.8981	β_{xyz}	10.6141		
αx 10^{-23}(esu)	-2.76	β_{tot} x 10^{-30} (esu)	1.01		

The dipole moment for the synthesized molecule was found to be 1.9456 (D). Total dipole polarizability was observed as -2.76 x 10^{-23} (esu). First hyperpolarizability tensors were observed -1.1238, 47.8623 and -1.3937 a.u along x, y and z-axis respectively (Table-6). So the first hyperpolarizability tensor along y-axis (with positive direction) is found larger than the first hyperpolarizability tensors along x and z-axis (with negative directions) respectively. Total first hyperpolarizability value was examined as 1.01 x 10^{-30} (esu). On comparing our results with standard urea molecule [48, 49], the total dipole moment of the synthesized molecule was observed 1.42 times larger than the urea dipole moment (1.3732D). First hyperpolarizability was observed 2.72 times greater than the urea (β=0.372x10^{-30} esu). This greater value of first order hyperpolarizability is because of the presence of weakly activating two methyl groups and one ethyl group attached to the benzene ring directly and through CO_2 molecule respectively. The second hyperpolarizability tensor along x direction was found to be -11704.5324 which are higher than their y and z directions (Table-6). The total second hyperpolarizability value of the synthesized molecule is examined at -2.10 x 10^{-28} esu. From above discussion, it is apparent that the synthesized molecule shows the evidence of tunable NLO performance and may have potential applications in the development of NLO materials.

Molecular electrostatic potential (MEP)

MEP is a thoroughly defined expectation quantity which is used to draw the three dimensional plot of total electron density. MEP is well–known for its role in terms of describing the reactivity of a chemical system by forecasting various nucleophilic and electrophilic sites in target molecule [50]. During MEP mapping, two basic regions red and blue appear which correspond to the extreme value of electrostatic potential. The nucleophilic site with positive potential is indicated by blue color, while negative potential site favored for electrophilic attack is indicated by red. Electrostatic potential is enhanced in the order of red < orange < yellow < green < blue [51]. To anticipate the electrostatic potential areas and physiochemical features of the investigated molecule, DFT computations were executed on the optimized geometry by M06-2X/6-311+G(d,p) level of theory and pictographic display is shown in Fig. 5.

From Fig. 5, it can be seen that the most negative potential region red is located over oxygen atom. Thus oxygen atom of SO_2 and CO_2 group is the most favorable site for electrophilic attack in synthesized molecule. On the other hand, blue color is mostly positioned over carbon and hydrogen atoms which imply that nucleophile will preferably attack on these sites. The average of the two extreme value of electrostatic potential (red and blue) is represented by green region which is confined over hydrogen atoms. The locations of halfway potential between the extremes (red and blue) and mean (green) is indicated by yellow color and located over S atom in synthesized molecule.

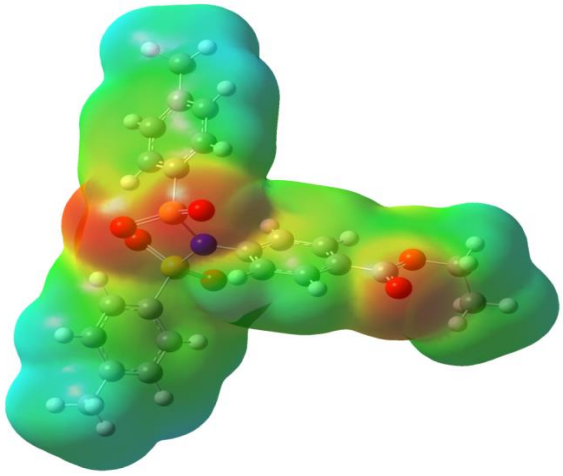

Fig. 5: Electrostatic potential mapping on the electron density (iso value = 0.02)

Thermodynamic parameters

The connection among the standard statistical thermodynamic functions like temperature, molar entropy, enthalpy, and heat capacity were studied at 100-1000 K using M06-2X/6311+g(d,p) level of theory in gas phase and results are tabulated in Table-7.

Table-7: Thermodynamic parameters with various temperatures.

T (K)	S_m^0 *(J/mol.K)*	$C_{p,m}^0$ *(J/mol.K)*	H_m^0 *(kJ/mol)*
100	**523.43**	**220.21**	**14.02**
200	**718.82**	**358.91**	**43.00**
298	**887.66**	**496.02**	**84.95**
300	**890.74**	**498.58**	**85.87**
400	**1052.55**	**629.93**	**142.44**
500	**1205.47**	**741.05**	**211.17**
600	**1348.82**	**830.92**	**289.93**
700	**1482.54**	**903.4**	**376.77**
800	**1607.17**	**962.63**	**470.17**
900	**1723.47**	**1011.72**	**568.96**
1000	**1832.26**	**1052.91**	**672.25**

Molecular energies produced form translational, rotational and vibrational motion of the molecules is transformed into standard heat capacities, entropies and enthalpy changes. Table-7 indicates that at any temperature from 100.00 to

1000.00 K, standard enthalpy, heat capacities and entropy changes also increases due to increase in the intensity of the molecular vibration. The correlations graphs are displayed in Fig. 6. These acquired thermodynamic properties data provide supportive information for further study on the synthesized molecule.

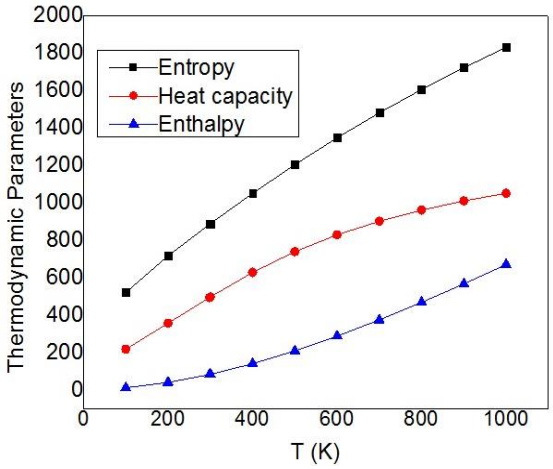

Fig. 6: Graphical representation of thermodynamic parameters with various temperatures.

Conclusions

In the present work, experimental conditions for the synthesis of Ethyl 4-[*N*,*N*-*bis*(*p*-toluenesulfonyl)]amino-benzoate have been disclosed. The characterization of the chemical structure was carried out through X-ray crystallographic technique. The XRD studies suggest that the crystal structure is of monoclinic shape with space group *P21/n*. Good correspondence is found between XRD crystal structure and DFT optimized structures data. NBO probe explored stronger hyper conjugative interactions which are mainly responsible for the stability of the derivatives. The NBO analysis revealed that the σ(C52-H55) and LP(3)O5 interaction gives the strongest stabilization to the molecule. The greater values of the calculated dipole moment and first order hyperpolarizability from the reference molecule (urea) indicate that the investigated molecule show the evidence of promising NLO performance and may have potential applications in the development of NLO materials. The global reactivity parameters indicated the larger hardness and less softness values. These findings reveal that the molecule might be stable. The MEP map shows that the negative potential sites are located on electronegative oxygen atom while the positive potential sites are found around the hydrogen atoms. The connection among the standard statistical thermodynamic functions and temperature reveals that the entropies, standard heat capacities and enthalpy changes increase with temperature because of increase in the intensity of the molecular vibration. Hence, we believe that this study reveals the interesting electronic properties of the synthesized molecule, which will be useful to experimental and theoretical details of further studies.

Conflict of interest

No conflicts declared.

Acknowledgements

Authors are thankful to Departamento de Química Fundamental, Instituto de Quimica, Universidade de São Paulo, Av. Prof. LineuPrestes, 748, São Paulo, 05508-000, Brazil for providing theoretical lab facilities for DFT study. A.A.C.B (grants #2015/01491-3 and 2014/25770-6) is thankful to Fundação de Amparo à Pesquisa do Estado de São Paulo for financial support. Moreover, Muhammad Khalid (grant#2017/1314) is thankful to HEC Islamabad Pakistan for financial support.

References

1. C. Hansch, P. G. Sammes and J. B. Taylor, *Comprehensive medicinal chemistry: the rational design, mechanistic study & therapeutic applications of chemical compounds*, Pergamon Pr. (1989).
2. M. Navia, Rational design of new immunosuppressive drugs, Transplant. Proc., Elsevier, 1999, pp. 1097-1098.
3. S. K. Mohamed, Synthesis of new sulfonamide drugs, *Afinidad* **57**, 451 (2000).
4. K. Bhusari, P. Khedekar, S. Umathe, R. Bahekar and A. R. R. Rao, Synthesis of 8-bromo-9-substituted-1, 3-benzothiazolo-[5, 1-b]-1, 3, 4-triazoles and their anthelmintic activity, *Indian J. Heterocycl. Chem.* **9**, 275 (2000).
5. S. Bhusare, R. Pawar and Y. Vibhute, Synthesis and antibacterial activity of some new 2-(substituted phenyl sulfonamido)-6-substituted benzothiazoles, *Indian J. Heterocycl. Chem.* **11**, 79 (2001).
6. B. Ahmed, S. Khan and T. Alam, Synthesis and antihepatotoxic activity of some heterocyclic compounds containing the 1, 4-dioxane ring system, *Die Pharmazie-An International Journal of Pharmaceutical Sciences* **58**, 173 (2003).
7. B. C. Shekar, K. Roy and A. De, Synthesis of some new p-toluene sulfonamido glutaramides, *Indian J. Heterocycl. Chem.* **10**, 237 (2001).
8. R. F. Borne, R. L. Peden, I. Waters, M. Weiner, R. Jordan and E. A. Coats, Anti-inflammatory

activity of para-substituted N-benzenesulfonyl derivatives of anthranilic acid, *J. Pharm. Sci.* **63**, 615 (1974).

9. J. Mun, A. A. Jabbar, N. S. Devi, S. Yin, Y. Wang, C. Tan, D. Culver, J. P. Snyder, E. G. Van Meir and M. M. Goodman, Design and in Vitro Activities of N-Alkyl-N-[(8-R-2, 2-dimethyl-2 H-chromen-6-yl) methyl] heteroarylsulfonamides, Novel, Small-Molecule Hypoxia Inducible Factor-1 Pathway Inhibitors and Anticancer Agents, *J. Med. Chem.* **55**, 6738 (2012).
10. N. S. El-Sayed, E. R. El-Bendary, S. M. El-Ashry and M. M. El-Kerdawy, Synthesis and antitumor activity of new sulfonamide derivatives of thiadiazolo [3, 2-a] pyrimidines, *Eur. J. Med. Chem.* **46**, 3714 (2011).
11. M. Mirian, A. Zarghi, S. Sadeghi, P. Tabaraki, M. Tavallaee, O. Dadrass and H. Sadeghi-aliabadi, Synthesis and cytotoxic evaluation of some novel sulfonamidederivativesagainst a few human cancer cells, *Iranian journal of pharmaceutical research: IJPR* **10**, 741 (2011).
12. E. Clercq, New developments in anti-HIV chemotherapy, *Curr. Med. Chem.* **8**, 1543 (2001).
13. W. R. Roush, S. L. Gwaltney, J. Cheng, K. A. Scheidt, J. H. McKerrow and E. Hansell, Vinyl sulfonate esters and vinyl sulfonamides: potent, irreversible inhibitors of cysteine proteases, *J. Am. Chem. Soc.* **120**, 10994 (1998).
14. M. Mengelers, P. Hougee, L. Janssen and A. Van Miert, Structure-activity relationships between antibacterial activities and physicochemical properties of sulfonamides, *J. Vet. Pharmacol. Ther.* **20**, 276 (1997).
15. J. F. O'Connell and H. Rapoport, 1-Benzenesulfonyl-and 1-p-toluenesulfonyl-3-methylimidazolium triflates: efficient reagents for the preparation of arylsulfonamides and arylsulfonates, *J. Org. Chem.* **57**, 4775 (1992).
16. J. M. Baskin and Z. Wang, A mild, convenient synthesis of sulfinic acid salts and sulfonamides from alkyl and aryl halides, *Tetrahedron Lett.* **43**, 8479 (2002).
17. H. S. Nalwa and S. Miyata, *Nonlinear optics of organic molecules and polymers*, CRC press. (1996).
18. F. Ghebremichael, M. Kuzyk and H. Lackritz, Nonlinear optics and polymer physics, *Prog. Polym. Sci.* **22**, 1147 (1997).
19. K. Clays and B. J. Coe, Design strategies versus limiting theory for engineering large second-order nonlinear optical polarizabilities in charged organic molecules, *Chem. Mater.* **15**, 642 (2003).
20. B. J. Coe, L. A. Jones, J. A. Harris, B. S. Brunschwig, I. Asselberghs, K. Clays and A. Persoons, Highly unusual effects of π-conjugation extension on the molecular linear and quadratic nonlinear optical properties of ruthenium (II) ammine complexes, *J. Am. Chem. Soc.* **125**, 862 (2003).
21. B. J. Coe, L. A. Jones, J. A. Harris, B. S. Brunschwig, I. Asselberghs, K. Clays, A. Persoons, J. Garín and J. Orduna, Syntheses and spectroscopic and quadratic nonlinear optical properties of extended dipolar complexes with ruthenium (II) ammine electron donor and N-methylpyridinium acceptor groups, *J. Am. Chem. Soc.* **126**, 3880 (2004).
22. L. R. Dalton, A. W. Harper and B. H. Robinson, The role of London forces in defining noncentrosymmetric order of high dipole moment–high hyperpolarizability chromophores in electrically poled polymeric thin films, *Proceedings of the National Academy of Sciences* **94**, 4842 (1997).
23. Y. Shi, C. Zhang, H. Zhang, J. H. Bechtel, L. R. Dalton, B. H. Robinson and W. H. Steier, Low (sub-1-volt) halfwave voltage polymeric electro-optic modulators achieved by controlling chromophore shape, *Science* **288**, 119 (2000).
24. E. K. Gross and R. M. Dreizler, *Density functional theory*, Springer Science & Business Media. (2013).
25. M. J. Frisch, G. W. Trucks, H. B. Schlegel, G. Scuseria, M. A. Robb, J. R. Cheeseman, G. Scalmani, V. Barone, B. Mennucci, G. Petersson, H. Nakatsuji, M. Caricato, X. Li, H. P. Hratchian, A. F. Izmaylov, J. Bloino, G. Zheng, J. L. Sonnenberg, M. Hada, M. Ehara, K. Toyota, R. Fukuda, J. Hasegawa, M. Ishida, T. Nakajima, Y. Honda, O. Kitao, H. Nakai, T. Vreven, J. A. Montgomery, J. E. Peralta, F. Ogliaro, M. Bearpark, J. J. Heyd, B. E, K. N. Kudin, V. N. Staroverov, R. Kobayashi, J. Normand, K. Raghavachari, A. Rendell, J. C. Burant, S. S. Iyengar, J. Tomasi, M. Cossi, N. Rega, J. M. Millam, M. Klene, J. E. Knox, J. B. Cross, V. Bakken, C. Adamo, J. Jaramillo, R. Gomperts, R. E. Stratmann, O. Yazyev, A. J. Austin, R. Cammi, C. Pomelli, J. W. Ochterski, R. L. Martin, K. Morokuma, V. J. Zakrzewski, G. A. Voth, P. Salvador, J. J. Dannenberg, S. Dapprich, A. D. Daniels, O. Farkas, J. B. Foresman, J. V. Ortiz, J. Cioslowski and D. J. Fox, D. 0109, Revision D. 01, Gaussian, *Inc., Wallingford, CT* (2009).
26. Avagadro, *http://avogadro.cc/wiki/Main_Page*.
27. ChemCraft, *http:// www. chemcraftprog. com.*

28. A. Frisch, A. Nielsen and A. Holder, Gaussview users manual, *Gaussian Inc., Pittsburgh, PA* (2000).
29. S. Bruker, APEX2 and SAINT, *Bruker AXS Inc., Madison, Wisconsin, USA* (2007).
30. G. M. Sheldrick, A short history of SHELX, *Acta Crystallogr. Sect. A: Found. Crystallogr.* **64**, 112 (2008).
31. L. J. Farrugia, WinGX and ORTEP for Windows: an update, *J. Appl. Crystallogr.* **45**, 849 (2012).
32. A. L. Spek, Structure validation in chemical crystallography, *Acta Crystallogr. Sect. D. Biol. Crystallogr.* **65**, 148 (2009).
33. D. R. Lide, A survey of carbon-carbon bond lengths, *Tetrahedron* **17**, 125 (1962).
34. M. Adeel, A. A. Braga, M. N. Tahir, F. Haq, M. Khalid and M. A. Halim, Synthesis, X-ray crystallographic, spectroscopic and computational studies of aminothiazole derivatives, *J. Mol. Struct.* **1131**, 136 (2017).
35. M. N. Tahir, M. Khalid, A. Islam, S. M. A. Mashhadi and A. A. Braga, Facile synthesis, single crystal analysis, and computational studies of sulfanilamide derivatives, *J. Mol. Struct.* **1127**, 766 (2017).
36. M. Snehalatha, C. Ravikumar, I. H. Joe, N. Sekar and V. Jayakumar, Spectroscopic analysis and DFT calculations of a food additive Carmoisine, *Spectrochim. Acta. A Mol. Biomol. Spectrosc.* **72**, 654 (2009).
37. S. Gunasekaran, R. A. Balaji, S. Kumeresan, G. Anand and S. Srinivasan, Experimental and theoretical investigations of spectroscopic properties of N-acetyl-5-methoxytryptamine, *Can. J. Anal. Sci. Spectrosc* **53**, 149 (2008).
38. S. S. Amiri, S. Makarem, H. Ahmar and S. Ashenagar, Theoretical studies and spectroscopic characterization of novel 4-methyl-5-((5-phenyl-1, 3, 4-oxadiazol-2-yl) thio) benzene-1, 2-diol, *J. Mol. Struct.* **1119**, 18 (2016).
39. M. Khalid, M. Ali, M. Aslam, S. H. Sumrra, M. U. Khan, N. Raza, N. Kumar and M. Imran, Frontier molecular, Natural bond orbital, UV-Vis spectral stduy, Solvent influence on geometric parameters, Vibrational frequencies and solvation energies of 8-Hydroxyquinoline, *Int. J. Pharma. Sci. and Res.*, **8**, 457 (2017).
40. R. G. Parr, L. V. Szentpaly and S. Liu, Electrophilicity index, *J. Am. Chem. Soc.* **121**, 1922 (1999).
41. R. G. Parr, R. A. Donnelly, M. Levy and W. E. Palke, Electronegativity: the density functional viewpoint, *J. Chem. Phys.* **68**, 3801 (1978).
42. P. K. Chattaraj, U. Sarkar and D. R. Roy, Electrophilicity index, *Chem. Rev.* **106**, 2065 (2006).
43. A. Lesar and I. Milošev, Density functional study of the corrosion inhibition properties of 1, 2, 4-triazole and its amino derivatives, *Chem. Phys. Lett.* **483**, 198 (2009).
44. M. R. S. A. Janjua, Nonlinear optical response of a series of small molecules: quantum modification of π-spacer and acceptor, *J. Iran. Chem. Soc.* 1-14 (2017).
45. M. R. S. A. Janjua, First-Principle Study on the Effect of Pi-Spacers on Small Molecule Acceptors: Quantum Design of Organic Solar Cells and NLO Compounds, *J. Cluster Sci.* **28**, 2419 (2017).
46. M. R. S. A. Janjua, M. U. Khan, B. Bashir, M. A. Iqbal, Y. Song, S. A. R. Naqvi and Z. A. Khan, Effect of π-conjugation spacer (C C) on the first hyperpolarizabilities of polymeric chain containing polyoxometalate cluster as a side-chain pendant: A DFT study, *Comp. Theor. Chem.* **994**, 34 (2012).
47. M. R. S. A. Janjua, M. Amin, M. Ali, B. Bashir, M. U. Khan, M. A. Iqbal, W. Guan, L. Yan and Z. M. Su, A DFT Study on The Two-Dimensional Second-Order Nonlinear Optical (NLO) Response of Terpyridine-Substituted Hexamolybdates: Physical Insight on 2D Inorganic–Organic Hybrid Functional Materials, *Eur. J. Inorg. Chem.* **2012**, 705 (2012).
48. P. N. Prasad and D. J. Williams, *Introduction to nonlinear optical effects in molecules and polymers*, Wiley New York etc. (1991).
49. R. P. Singh, K. Singh, S. Sharma and A. Sethi, Synthesis, crystal structure, conformational analysis, nonlinear optical property and computational study of novel pregnane derivatives, *J. Mol. Struct.* **1095**, 125 (2015).
50. S. Demir Kanmazalp, E. Başaran, A. Karaküçük-Iyidoğan, E. E. Oruç-Emre and N. Dege, X-ray structures and spectroscopic properties of chiral thiosemicarbazides as studied by computational calculations, *Phosphorus, Sulfur, and Silicon and the Related Elements* 1-10 (2017).
51. G. Mahalakshmi and V. Balachandran, NBO, HOMO, LUMO analysis and vibrational spectra (FTIR and FT Raman) of 1-Amino 4-methylpiperazine using ab initio HF and DFT methods, *Spectrochim. Acta. A Mol. Biomol. Spectrosc.* **135**, 321 (2015).